

# Hydrogen effects in gamma titanium aluminides

J. HADDAD, D. ELIEZER

*Department of Materials Engineering, Ben-Gurion University, Beer-Sheva, Israel*

The results of X-ray diffraction studies on Ti–48Al–1V at % (Ti–48–1) are reported. The objective of this study is to investigate the effects of hydrogen on phase changes and hydride formation in these alloys. Hydrogen-induced cracking was found to occur as a result of hydrogen charging. The cracking appears after the hydride phase formation and is observed to be dispersed throughout the material. The hexagonal hydride formed is unlike any previously reported titanium hydride. The hydride exhibits an 8% volume contraction compared to Ti<sub>3</sub>Al which is made up of a 10% contraction in the *a*-direction, and a 12.5% expansion in the *c*-direction.

## 1. Introduction

Alloys based on TiAl are of considerable interest because of their relatively low density and good elevated temperature strength, although they typically exhibit very low ductility at room temperature (generally < 1% elongation). An understanding of ductility and fracture behaviour is still emerging [1–4], as is a knowledge of environmental effects such as hydrogen embrittlement [5–7]. The objective of this study is to investigate the effects of hydrogen on phase changes and hydride formation in the Ti–48Al–1V at % alloys (Ti–48–1).

## 2. Experimental procedure

The hydrogen charging and X-ray diffraction studies were carried out on samples of Ti–48–1 cut from a plate using an electric spark erosion machine. The X-ray and metallography specimens were cathodically hydrogen charged at room temperature for various durations with an 100 mA cm<sup>-2</sup> current density in an H<sub>2</sub>SO<sub>4</sub> solution with 50 mg of NaAsO<sub>2</sub> per litre added as a hydrogen recombination poison. The charged specimens were sealed in evacuated tubes and heat treated at different temperatures for one hour. Other specimens were also sealed in evacuated tubes and heat treated at 100 °C for different lengths of time.

The X-ray diffraction measurements were used to determine the phases present and their lattice parameters before and after charging. A computerized Philips X-ray diffractometer with a Cu-anode and a scintillation detector was used in the diffraction studies.

## 3. Results and discussion

In the as-received (AR) material, a two-phase structure was observed consisting of TiAl ( $\gamma$ ) and Ti<sub>3</sub>Al ( $\alpha_2$ ) (Fig. 1). This structure was made up of alternate layers of lamellar  $\gamma$  and  $\alpha_2$  plates.

After hydrogen charging, grain boundary and intergranular cracks were present (Fig. 2). An X-ray diffraction pattern from an uncharged specimen is shown in Fig. 3. In this case, two different phases were observed:  $\gamma$  (TiAl) with an f.c.t. structure, and approximately 6–8%  $\alpha_2$  (Ti<sub>3</sub>Al) phase with an h.c.p. structure. The lattice parameters of the  $\gamma$  phase are  $a = 0.400$  nm,  $c = 0.406$  nm, and of the  $\alpha_2$  are  $a = 0.578$  nm and  $c = 0.464$  nm. An X-ray pattern from the Ti–48–1 alloy taken after various durations of hydrogen charging is shown in Fig. 4. The  $\gamma$  peaks shift slightly toward smaller diffraction angle values compared to the uncharged material. After some hours of charging, the peaks for the  $\alpha_2$  phase exhibit broadening and a new phase begins to appear throughout the material. After 3 h of charging, all the peaks of the  $\alpha_2$  phase disappear and the  $\gamma$  peak intensities begin to change.

The bulk hydrogen contents before and after charging, as measured by a Leco-RH402 instrument, are given in Table I. The new phase was determined to be a hydride. X-ray diffraction was used to determine the structural and lattice parameters of this phase. The X-ray diffraction data shows that the structure of the

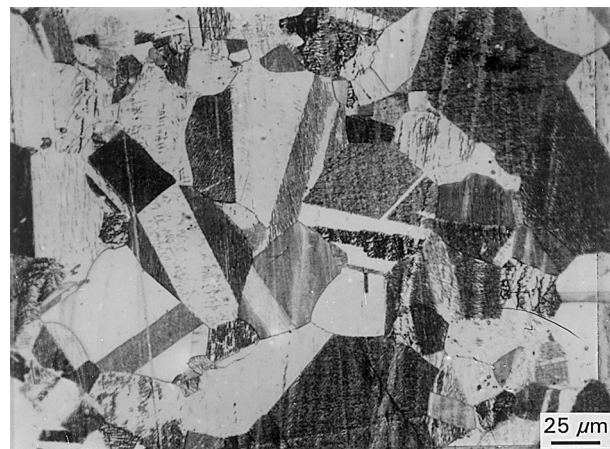


Figure 1 Metallographic micrograph of the as-received Ti–48Al–1V (at %) alloy.



Figure 2 Scanning electron micrograph of the Ti-48Al-1V (at %) alloy after hydrogen charging for 88 h. Cracks around boundaries and intergranular cracks induced by hydrogen can be noted.

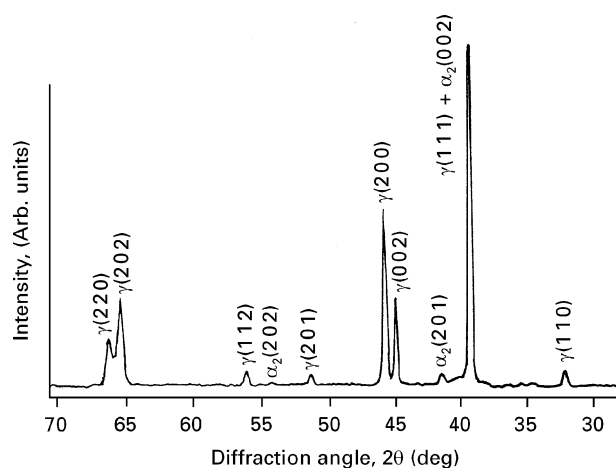


Figure 3 X-ray diffraction pattern of as-received Ti-48Al-1V (at %) alloy.

new phase is hexagonal with a  $c/a$  ratio  $\approx 1$ . The lattice parameters and specific volume are different from either  $\gamma$  or  $\alpha_2$  (see Table II). The volume of the new phase exhibits an 8% contraction compared to  $\alpha_2$  (see Table II). This arises from a 10% contraction of the  $a$ -parameter with respect to  $\alpha_2$ , and a 12.5% expansion of the  $c$ -parameter compared to  $\alpha_2$ .

Fig. 5 shows the X-ray diffraction patterns from the Ti-48-1 alloy taken after 24 h of charging and after various ageing times at room temperature. During ageing following cathodic charging, some of the  $\alpha_2$  peak broadening disappears and the peaks of  $\gamma$  shift toward higher diffraction angles, the new peaks become sharper and more intense. This shifting of the  $\gamma$  peaks indicates an increase in the lattice parameters during charging (Table II). However, the decrease in the lattice parameters on ageing is probably due to loss of hydrogen from the specimens. Fig. 6 shows the X-ray diffraction patterns from the alloys taken after 36 h of charging at room temperature and after ageing at various temperatures for 1 h. During temperature ageing, the hydride concentration decreases, and finally disappears after 1 h of ageing at 300 °C. All the peaks in the patterns in Fig. 6 (a-f) were identified as belonging to only the  $\gamma$  and  $\alpha_2$  phases. To confirm that

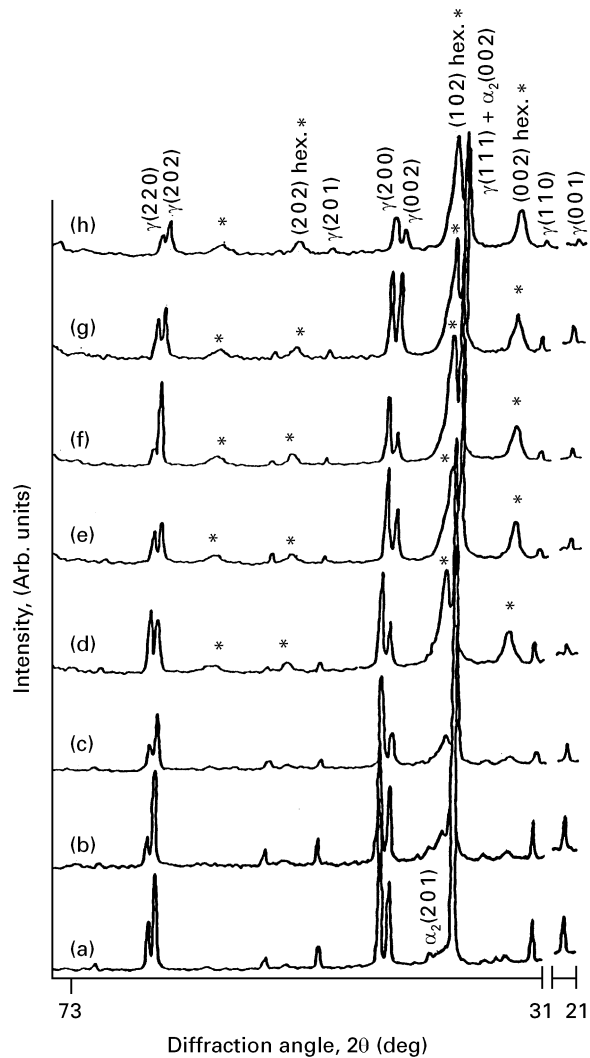


Figure 4 X-ray diffraction patterns of Ti-48Al-1V (at %) alloy after charging for various lengths of time (new peaks that appear throughout the pattern are marked as \*) The lengths of time investigated were (a) as received, (b) 1 h, (c) 2 h, (d) 3 h, (e) 5 h, (f) 8 h, (g) 12 h and (h) 18 h.

TABLE I Hydrogen content in Ti-48-1 before and after charging and during ageing

Ageing Time (h) →	0	1	3	12	24	120	240
Charging Time (h) ↓							
0	53 ± 10	—	—	—	—	—	—
12	111 ± 13	82	75	—	75 ± 11	—	—
18	120 ± 25	97	85	—	80 ± 13	—	—
36	130 ± 30	97	86	—	78 ± 15	—	—
88	139 ± 32	107	88	—	84 ± 18	—	—

the AR samples have no hydrogen before charging, this material was sealed in a vacuum and then annealed at 700 °C for 4 h (Fig. 6a). We can see that an  $\alpha_2$  (200) peak appears in Fig. 6a that is not present in Fig. 3. This is proof that a little hydrogen is absorbed during the production process.

Fig. 7 shows the X-ray diffraction patterns from the samples taken after 36 h of charging at room temperature and after various ageing periods at 100 °C. It is easy to see that during ageing at 100 °C the amount of

TABLE II Comparison of the lattice parameters of the phases in Ti-48-1 before and after charging

	Before charging		f.c.t.-TiAl( $\gamma$ )	After charging and 10 days ageing	
	h.c.p.-Ti <sub>3</sub> Al( $\alpha_2$ )			TiA( $\gamma$ )	Hexagonal phase hydride
	This study	Gao <i>et al.</i> [15]			
$a$ (nm)	0.578	0.578	0.400	0.401	0.522
$c$ (nm)	0.464	0.467	0.406	0.407	0.525
$V$ (nm <sup>3</sup> )	0.134	0.135	0.065	0.065	0.124

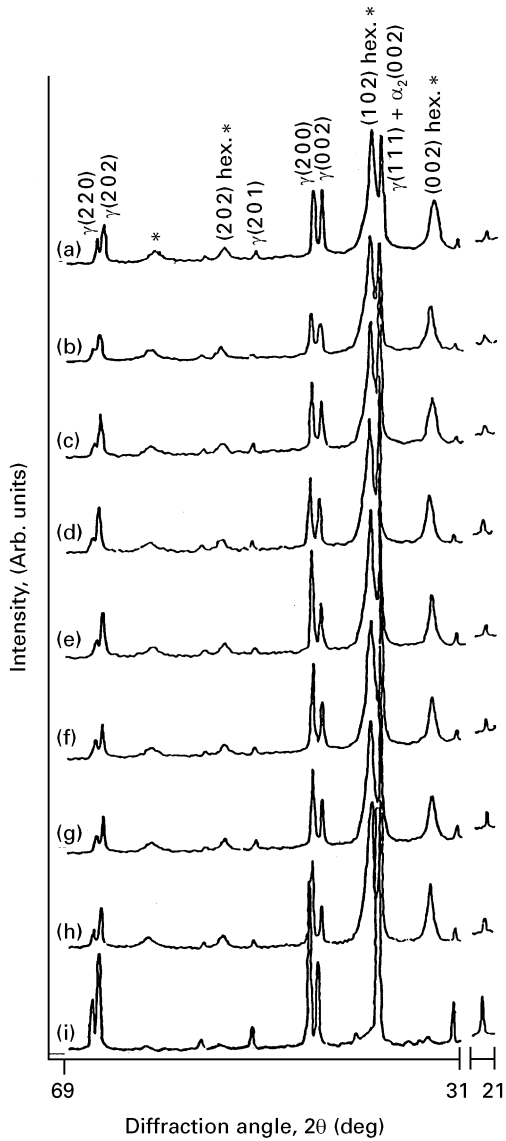


Figure 5 X-ray diffraction patterns of the Ti-48Al-1V (at %) alloy hydrogen charged for 24 h and aged at room temperature for the lengths of time of (a) 0 h, (b) 1.5 h, (c) 4 h, (d) 8 h, (e) 24 h, (f) 48 h, (g) 5 days, (h) 10 days for comparison (i) is the as received material.

the hydride decreases and that it decomposes at 100 °C after 4 h ageing (Fig. 7). From Figs 6 and 7, we can see that, as the hydrogen diffuses out of the specimen during heating and over time, the diffraction peaks of the hydride are shifted toward higher diffraction angles as is shown in Fig. 6(b–d) and also Fig. 7(a–c), whilst the diffraction peaks of the  $\alpha_2$  phase begin to reappear throughout the pattern. It is

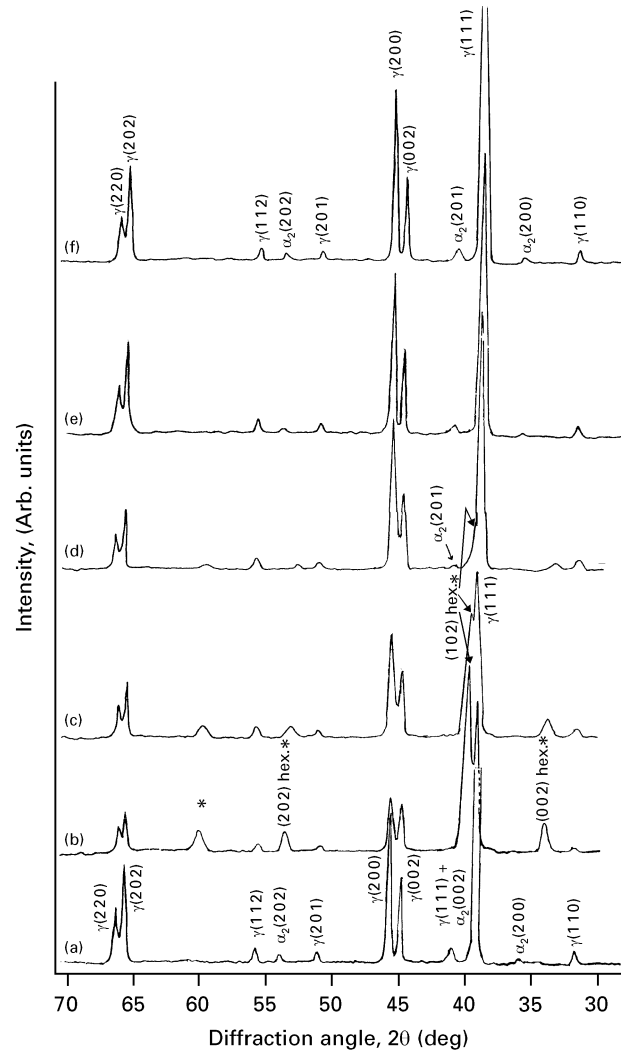


Figure 6 X-ray diffraction patterns of the Ti-48Al-1V (at %) alloy. (a) As-received after heat treatment at 700 °C for 4 h. (b) Sample A after charging for 36 h at room temperature. (c) Sample B after ageing at 100 °C for 1 h. (d) Sample B after ageing at 200 °C for 1 h. (e) Sample B after ageing at 300 °C for 1 h. (f) Sample B after ageing at 600 °C for 1 h.

probable that the  $\alpha_2$  phase converts into the hydride during hydrogen charging and is re-formed when the hydrogen diffuses out during heating.

Three types of titanium hydrides have been reported in literature:  $\delta$ ,  $\epsilon$ , and  $\gamma$ . The  $\delta$  hydride forms in the composition range from TiH<sub>1.5</sub> to TiH<sub>1.99</sub> and has a CaF<sub>2</sub> structure, with metal atoms on an f.c.c. lattice and hydrogen atoms randomly occupying tetrahedral

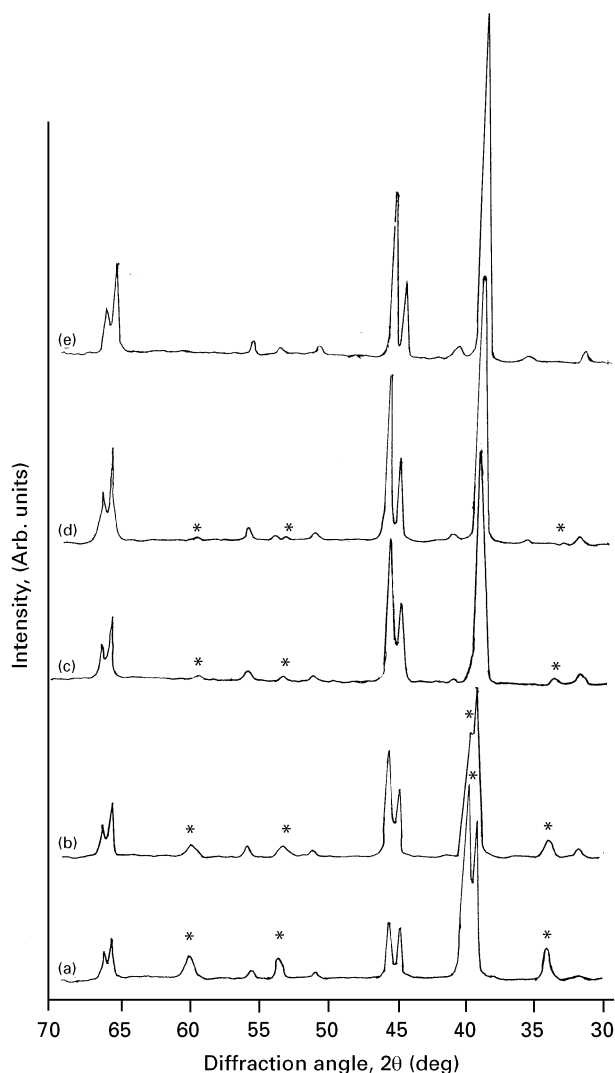


Figure 7 X-ray diffraction patterns of the Ti-48Al-1V (at %) alloy: (a) As-received after heat treatment at 700 °C for 4 h and charging for 36 h at room temperature. (b) Sample A after ageing at 100 °C for 1 h. (c) Sample A after ageing at 100 °C for 2 h. (d) Sample A after ageing at 100 °C for 3 h. (e) Sample A after ageing at 100 °C for 4 h.

interstitial sites [8–11]. At higher hydrogen concentrations,  $\text{TiH}_2$ , the f.c.s. ( $c/a < 1$ )  $\epsilon$  hydride phase is formed below 310 °K (583 °C) [9–12]. The  $c/a$  ratio decreases with decreasing temperatures until it reaches and maintains a minimum value of 0.943 below 80 °K (353 °C) [12]. The f.c.c. to tetragonal,  $\delta \rightarrow \epsilon$  transformation is apparently diffusionless [9]. The metastable f.c.t.  $\gamma$  hydride forms from a solid solution of hydrogen with an h.c.p.  $\alpha$  matrix and a  $c/a$  value of 1.09 [13, 14] or 1.12 [16].

Legzdina *et al.* [17] have identified an f.c.c.  $\text{TiH}_2$  phase formed in single  $\gamma$  or  $\gamma + \alpha_2$  TiAl alloys after exposure to a 13.8 mPa hydrogen atmosphere at 650 °C for 100 h. In addition Jia Gao *et al.* [18] have identified a tetragonal hydride formed during cathodic charging at room temperature.

In the present work the hydride phase has a hexagonal structure (Table II), and is quite unlike any of the reported titanium hydrides; it may well be that it is a  $(\text{Ti-Al}) \times \text{H}$  phase. The new peaks exhibit a non-symmetric profile, indicating a non-uniform hydrogen content that probably causes a non-uniform expansion of the material.

## 4. Conclusions

(i) Hydrogen induced cracking occurs as a result of hydrogen charging. The cracking appears after the hydride phase is observed to be dispersed throughout the material.

(ii) The X-ray peaks of the  $\alpha_2$  phase exhibit some broadening after hydrogen charging. The  $\gamma$  matrix shows a small lattice expansion after hydrogen charging, which decreases somewhat on subsequent ageing.

(iii) The hexagonal hydride formed is unlike any previously reported titanium hydride. The hydride exhibits an 8% volume contraction compared to  $\alpha_2$ , made up of a 10% contraction in the  $a$ -direction, and a 12.5% expansion in the  $c$ -direction.

(iv) The hydride is stable at room temperature for long time periods (Fig. 5).

(v) There is little evidence of hydrides after ageing at 200 °C for 1 h, but the hydride decomposes at temperatures greater than 200 °C (Fig. 6).

(vi) The hydride decomposes at 100 °C after a period of 4 h or more (Fig. 7).

## References

1. R. L. FLEISCHER, D. M. DIMIDUK and H. A. LIPSITT, *Ann. Rev. Mater. Sci.* **19** (1989) 231.
2. T. KAWABATA and O. IZUMI, in "High Temperature Aluminides and Intermetallics" edited by S. H. Wang, C. T. Liu, D. P. Pope and J. O. Stiegler (TMS-AIME, Warrendale, PA, 1990) p. 403.
3. Y. W. KIM and F. H. FROES, *ibid.* p. 465.
4. J. M. LARSEN, K. A. WILLIAMS, S. J. BALSONE and M. A. STUCKE, *ibid.* p. 521.
5. S. M. L. SASTRY, W. O. SOBOYEJO and R. J. LEDERICH, in "Summary Proceedings 3rd Workshop on Hydrogen Materials Interactions", NASP Joint Program, Office Workshop Pub. 1007, edited by H. G. Nelson (NASA-Ames, Moffett Field, CA 1990) p. 191.
6. N. S. STOLOFF, M. SHEA and A. CASTAGNA, in "Hydrogen Embrittlement of Intermetallic Compounds and their Composites in Environmental Effects on Advanced Materials", edited by R. E. Ricker and R. H. Jones (TMS, Warrendale, PA, 1991) p. 3.
7. A. W. THOMPSON, in "Environmental Effects in Titanium Aluminide Alloys, in Environmental Effects on Advanced Materials", edited by R. E. Ricker and R. H. Jones (TMS, Warrendale, PA, 1991) p. 21.
8. S. S. SIDHU, L. HEATON and D. D. ZAUBERIS, *Acta Crystallogr.* **9** (1957) 607.
9. H. L. YAKEL, Jr., *ibid.* **11** (1958) 46.
10. P. E. IRVING and C. J. BEEVERS, *Met. Trans.* **2** (1971) 613.
11. P. MILLENBACH and M. GIVON, *J. Less-Common Metals* **87** (1982) 179.
12. Z. M. AZARKH and P. I. GAVRILOV, *Soviet Phys. Cryst.* **15** (1970) 231.
13. H. NUMAKURA and M. KOIWA, *Acta Metall.* **32** (1984) 1799.
14. H. NUMAKURA, M. KOIWA, H. ASANO, H. MURATA and F. IZUMI, *Scripta Metall.* **20** (1986) 213.
15. MING GAO, J. BART and P. WEI, *ibid.* **24** (1990) 2135.
16. O. T. WOO and G. J. C. CARPENTER, *ibid.* **19** (1985) 931.
17. D. LEGZDINA, I. M. ROBERTSON and H. K. BIRNBAUM, *J. Mater. Res.* **6** (1991) 1230.
18. JIA GAO, YAN BIN WANG, WU-YANG CHU and CHIMEI HSIAO, *Scripta Metall.* **27** (1992) 1219.

Received 4 August 1994  
and accepted 13 February 1996